

Supporting Information

Pt-Ir nanocubes amplified lateral flow immunoassay for dehydroepiandrosterone

Huiyi Yang^a; Qiyi He^a; Junkang Pan^a; Ding Shen^a; Huanxin Xiao^a; Xiping Cui^{a,*};

Suqing Zhao^{a,*}

*^aDepartment of Pharmaceutical Engineering, School of Biomedical and
Pharmaceutical Sciences, Guangdong University of Technology, Guangzhou 510006,
People's Republic of China*

*Corresponding Author:

Prof. Suqing Zhao

Tel.: +86 15820258676

E-mail address: sqzhao@gdut.edu.cn (S.-Q. Zhao)

Dr. Xiping Cui

Tel.: +86 18813758818

E-mail address: cuixiping1989@163.com (X.-P. Cui)

E-mail addresses for other authors:

iyiuhgnay@163.com (H.-Y. Yang); chesto36@163.com (Q.-Y. He);

kang36576@163.com (J.-K. Pan); shending92@163.com (D. Shen);

hxq323723@163.com (H.-X. Xiao);

1. Materials and apparatus

1.1 Chemicals

Dehydroepiandrosterone (DHEA), dexamethasone (DXMS), β -estradiol (E2), cortisol (COR), dehydroepiandrosterone sulfate (DHEAs), progesterone (PRG), androstenedione (ASD), testosterone (TET), chloroplatinic acid hexahydrate ($\text{H}_2\text{PtCl}_6 \cdot 6\text{H}_2\text{O}$), potassium hexachloroiridate (K_2IrCl_6), ascorbic acid (AA), hexadecyltrimethylammonium chloride (CTAC), thiourea, NaN_3 and p-benzoquinone (PBQ) were obtained from Aladdin Co. Ltd. (Shanghai, China). Tetramethylbenzidine (TMB) was purchased from Sigma Co. Ltd. (St. Louis, USA). Goat-anti-rabbit IgG was purchased from Bioss Co. Ltd. (Shanghai, China). Polyclonal antibody against DHEA (pAb) was prepared in previous work¹. NC membrane (Sartorius CN140), wicking pad (H5072), adhesive backing (DB-6), sample pad (NJ-Y2) and conjugate pad (Ahlstrom 8964) were obtained from Jieyi Co. Ltd. (Shanghai, China). 3D-printed bracket was obtained in previous work.² PBS (0.01 M, pH 7.4) was prepared by using 8.0 g NaCl, 2.9 g Na_2HPO_4 and 0.2 g NaH_2PO_4 in 1000 mL distilled water. Artificial urine was prepared by using 2.5 g urea, 0.25 g Na_2HPO_4 , 0.25 g NaH_2PO_4 , 0.90 g NaCl, 0.30 g NH_4Cl , 0.20 g creatinine and 0.30 g sodium sulfite in 100 mL distilled water.³ All the chemicals used in this study were analytical reagent grade. Solutions were prepared with ultrapure water from a Millipore Milli-Q water purification system (Billerica, MA).

1.2 Apparatus

Transmission electron microscope (TEM) was conducted with a HT7700

microscope (Hitachi, Japan). Scanning electron microscopy (SEM) image was obtained through a SU8010 microscope (Hitachi, Japan). The ultraviolet spectrogram was measured by Lambda 25 UV/VIS spectrophotometer (PerkinElmer, USA). Zeta potential was determined by Zetasizer Nano ZS (Malvern, UK). Electron spin resonance (ESR) spectrum was measured by the use of a Bruker A300 spectrometer (Bruker, Germany).

Figure and table captions

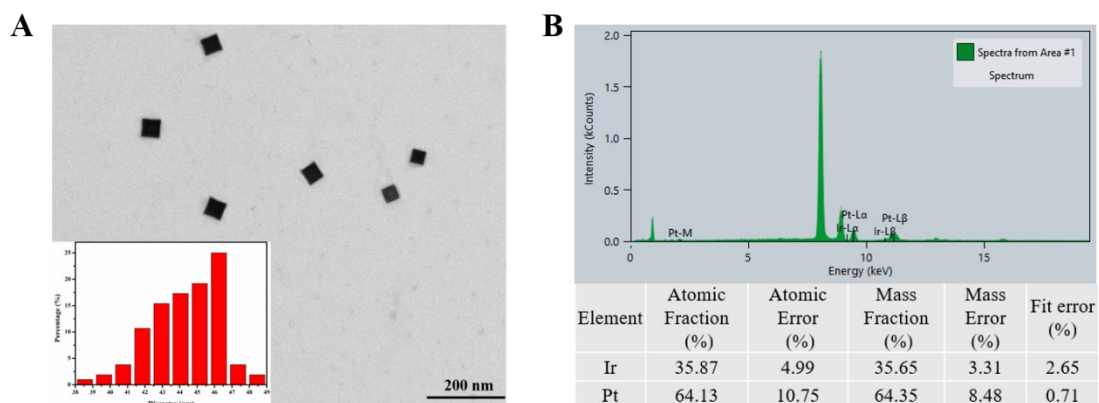


Fig. S1 (A) TEM image of PtNCs and the corresponding histogram of diameter; (B) EDX spectrum and element content of Pt-Ir NCs.

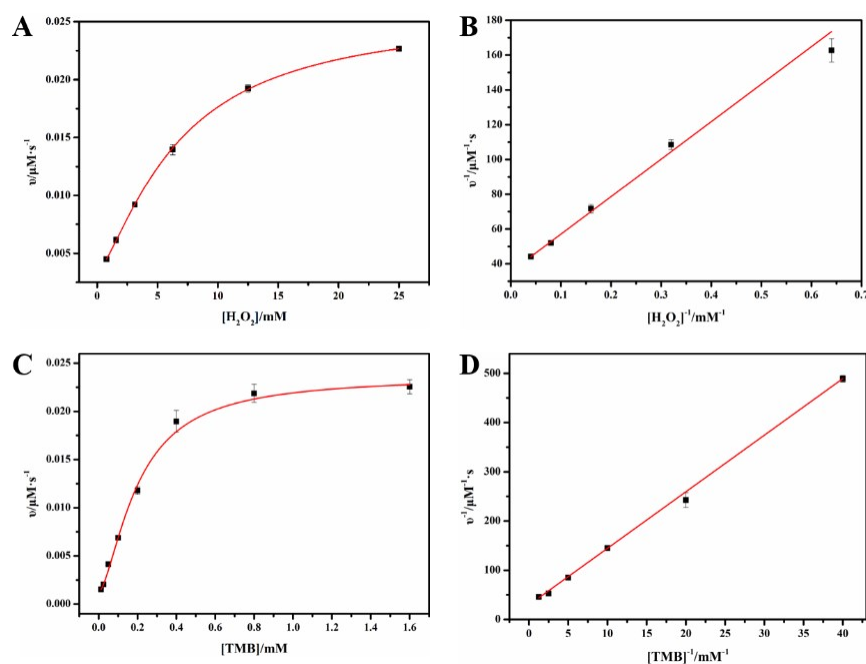


Fig. S2 Steady-state kinetic assay of Pt-Ir NCs. (A) H_2O_2 concentration and (C) TMB concentration dependence of initial reaction velocity (v); Double reciprocal plots between reaction velocity and (B) H_2O_2 concentration and (D) TMB concentration. Error bars denote the standard deviation ($n=3$).

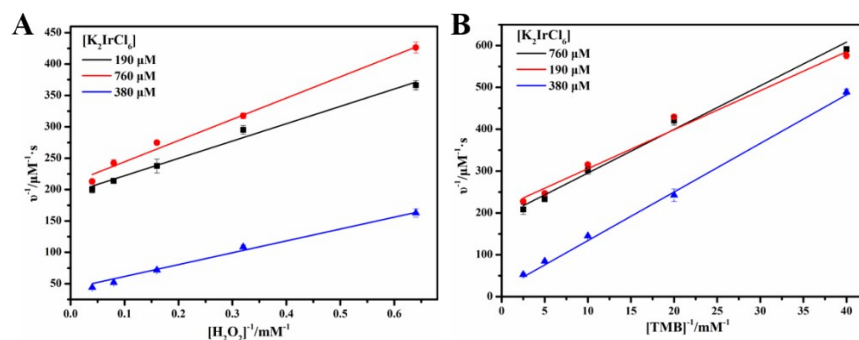


Fig. S3 Steady-state kinetic assay of Pt-Ir NCs prepared by different concentration of K_2IrCl_6 . Double reciprocal plots between reaction velocity and (A) H_2O_2 concentration and (B) TMB concentration. Error bars denote the standard deviation ($n=3$).

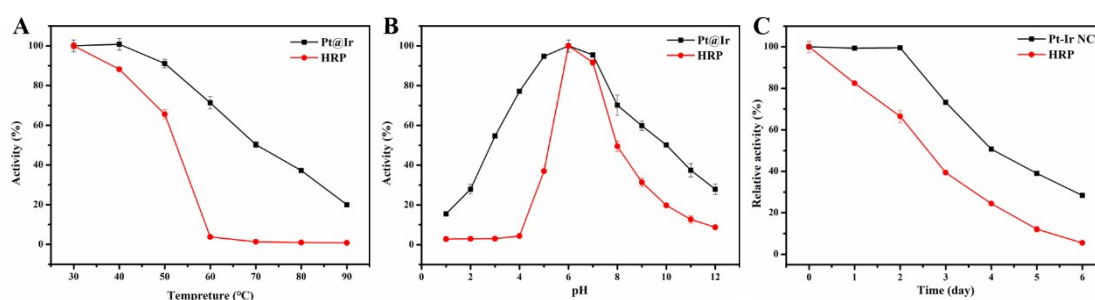


Fig. S4 Comparison of different types of stability under different conditions of Pt-Ir NCs and free HRP. (A) Chemical stability, (B) thermal stability and (C) storage stability at 37°C . Error bars denote the standard deviation ($n=3$).

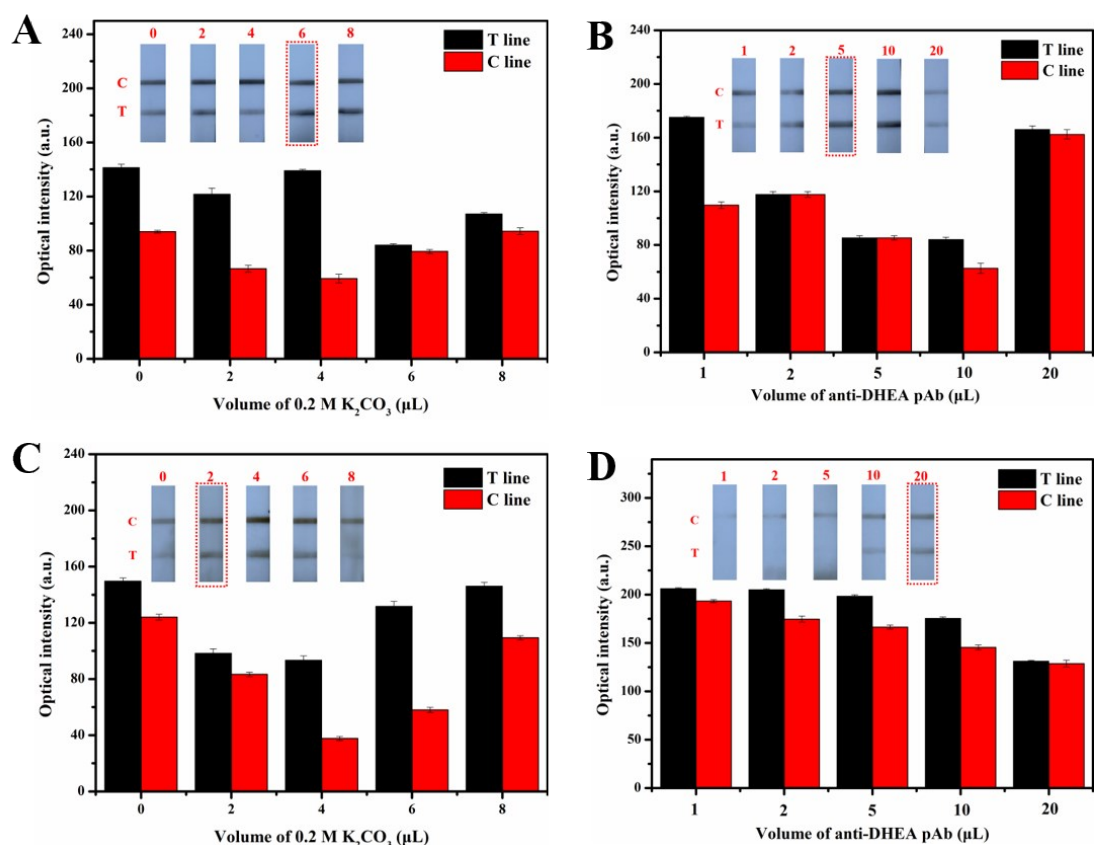


Fig. S5 Optimization of preparation parameters of the pAb-Pt-Ir and pAb-PtNCs probes. (A) The volume selection of 0.2 M K_2CO_3 (μL) performed in the pAb-Pt-Ir probe; (B) The volume selection of anti-DHEA pAb (μL) performed in the pAb-Pt-Ir probe; (C) The volume selection of 0.2 M K_2CO_3 (μL) performed in the pAb-PtNCs probe; (D) The volume selection of anti-DHEA pAb (μL) performed in the pAb-PtNCs probe.

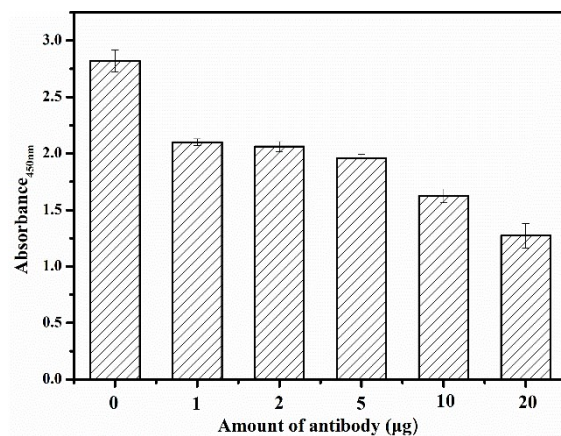


Fig. S6 Effect of amount of antibody on catalytic activity of Pt-Ir NCs.

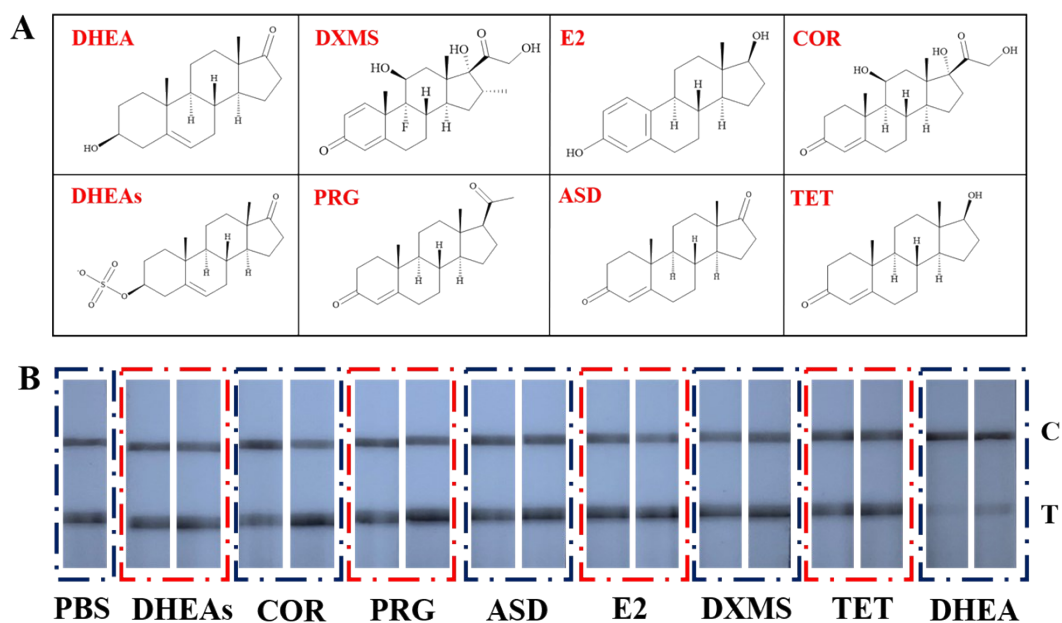


Fig. S7 (A) The structure of DHEA analogues; (B) Specificity research results of the Pt-Ir-LFIA immunosensor. 10,000 (right) and 1,000 ng·mL⁻¹ (left) of DHEA and its structural analogues were used in the assay. PBS buffer was used as negative control. All experiments were performed in triplicate.

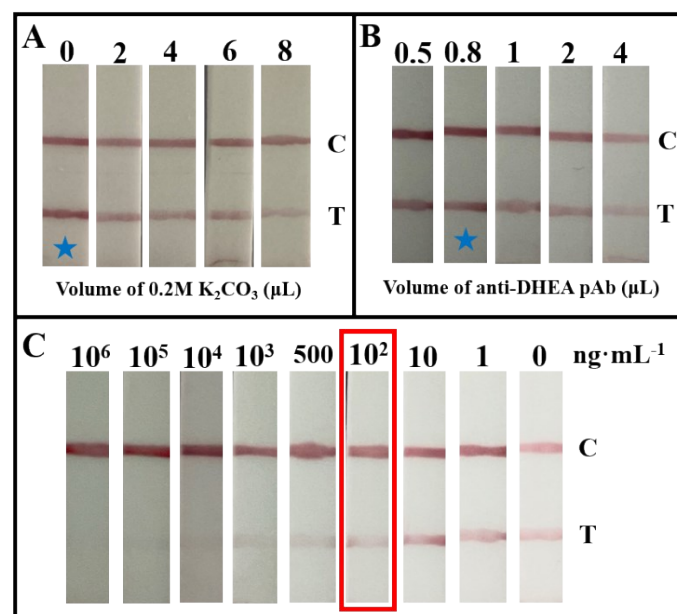


Fig. S8 Optimization of preparation parameters of the pAb-AuNPs. (A) The volume selection of 0.2 M K_2CO_3 (μL) performed in the pAb-AuNPs; (B) The volume selection of anti-DHEA pAb (μL) performed in the pAb-AuNPs probe; (C) Photographic results of AuNPs-LFIA for detection of DHEA by naked eyes.

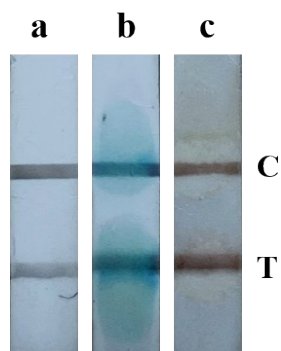


Fig. S9 Effects of different chromogenic reagent (a: none b: TMB and c: AEC) on the detection signal of Pt-Ir NCs.

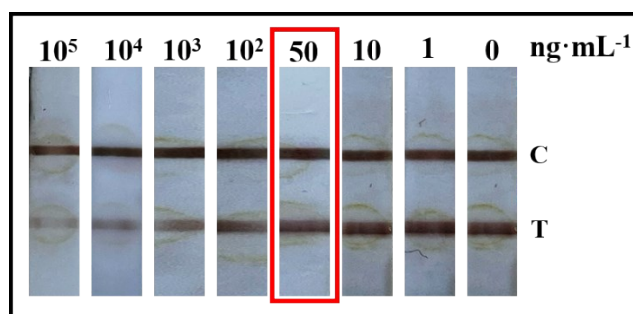


Fig. S10 Photographic results of enhanced PtNCs-based LFIA for DHEA by naked eyes; All experiments were performed in triplicate.

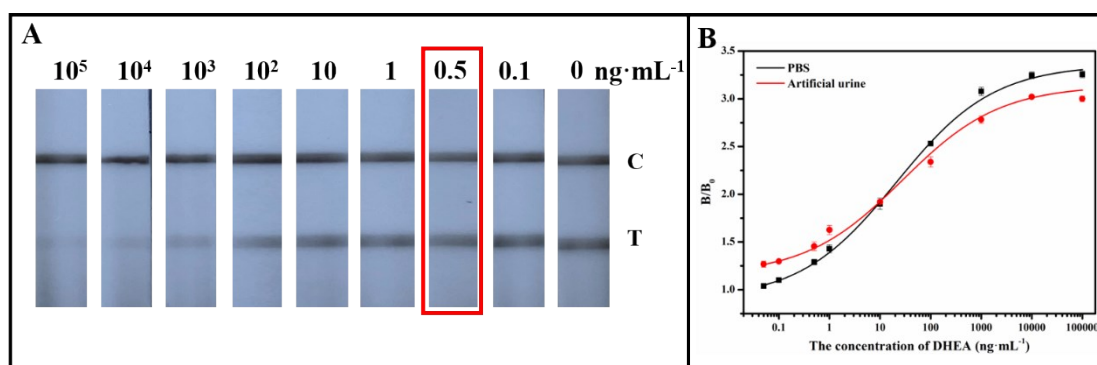


Fig. S11 (A)Photo images of Pt-Ir-based LFIA for DHEA in artificial urine; (B) Calibration curves in PBS buffer and artificial urine with Pt-Ir-LFIA. All experiments were performed in triplicate.

Table S1 Apparent steady-state kinetic parameters for Pt-Ir NCs and other metallic NPs peroxidase mimics.

Enzyme or Enzyme mimic	K_m (mM)		v_{max} ($10^{-8} \text{ M}\cdot\text{s}^{-1}$)		Ref
	H_2O_2	TMB	H_2O_2	TMB	
HRP	3.70	0.43	8.71	10.00	4
Platinum nanostructurs	769.00	0.12	185.00	126.00	5
PtNPs/GO	221.10	0.19	10.45	10.20	6
Pt ₂₀₀ -JP	9.344	0.719	12.49	51.33	7
Pt/PCN	7.37	1.06	23.50	23.12	8
Ag-Pt/rGO	1.25	3.24	16.7	20	9
Pd@Pt NDs	14	0.43	9	5.1	10
Au@Pt	4.076	2.431	6.013	4.425	11
PtNCs	17.20	2.96	3.27	6.52	This work
Pt-Ir NCs (190 μM)	7.01	2.28	3.62	10.70	This work
Pt-Ir NCs (760 μM)	6.2	1.84	2.95	9.50	This work
Pt-Ir NCs (380 μM)	4.13	0.38	2.60	3.4	This work

References

1. H. Yang, Q. He, Y. Chen, D. Shen, H. Xiao, S. A. Eremin, X. Cui and S. Zhao, *Mikrochim Acta*, 2020, **187**, 592.
2. Q. He, H. Yang, J. Pan, X. Cui, D. Shen, S. A. Eremin, Y. Fang and S. Zhao, *ACS Applied Bio Materials*, 2020, **3**, 8849-8856.
3. D. C. Kabiraz, K. Morita, K. Sakamoto, M. Takahashi and T. Kawaguchi, *Talanta*, 2018, **186**, 521-526.
4. J. Li, G. Zhang, L. Wang, A. Shen and J. Hu, *Talanta*, 2015, **140**, 204-211.
5. Z. Gao, M. Xu, L. Hou, G. Chen and D. Tang, *Anal Chim Acta*, 2013, **776**, 79-86.
6. L. N. Zhang, H. H. Deng, F. L. Lin, X. W. Xu, S. H. Weng, A. L. Liu, X. H. Lin, X. H. Xia and W. Chen, *Anal Chem*, 2014, **86**, 2711-2718.
7. X. Guo, Y. Suo, X. Zhang, Y. Cui, S. Chen, H. Sun, D. Gao, Z. Liu and L. Wang, *Analyst*, 2019, **144**, 5179-5185.
8. W. Shi, H. Fan, S. Ai and L. Zhu, *Sensors and Actuators B: Chemical*, 2015, **221**, 1515-1522.
9. L. Yao, F. Y. Kong, Z. X. Wang, H. Y. Li, R. Zhang, H. L. Fang and W. Wang, *Mikrochim Acta*, 2020, **187**, 410.
10. C. Ge, R. Wu, Y. Chong, G. Fang, X. Jiang, Y. Pan, C. Chen and J.-J. Yin, *Advanced Functional Materials*, 2018, **28**.
11. D. Wei, X. Zhang, B. Chen and K. Zeng, *Anal Chim Acta*, 2020, **1126**, 106-113.